AGU PUBLICATIONS

JGR

Journal of Geophysical Research: Solid Earth

RESEARCH ARTICLE
10.1002/2016JB013678

Key Points:
- Two distinct populations of amphiboles, with markedly different aluminum contents, are observed in the adakitic rocks
- Melts in equilibrium with the high-pressure amphiboles are of adakitic composition
- Amphibole composition that can be used to constrain the geochemical characteristics of pristine adakitic magmas

Supporting Information:
- Supporting Information S1
- Table S1

Correspondence to:
G.-J. Tang,
tanggj@gig.ac.cn

Citation:
Tang, G.-J., Q. Wang, D. A. Wyman, S.-L. Chung, H.-Y. Chen, and Z.-H. Zhao (2017), Genesis of pristine adakitic magmas by lower crustal melting: A perspective from amphibole composition, *J. Geophys. Res. Solid Earth*, *122*, 1934–1948, doi:10.1002/2016JB013678.

Received 25 OCT 2016
Accepted 5 MAR 2017
Accepted article online 7 MAR 2017
Published online 22 MAR 2017

Genesis of pristine adakitic magmas by lower crustal melting: A perspective from amphibole composition

Gong-Jian Tang[1,2], Qiang Wang[1,2], Derek A. Wyman[3], Sun-Lin Chung[4,5], Hong-Yi Chen[6], and Zhen-Hua Zhao[7]

[1]State Key Laboratory of Isotope Geochemistry, Guangzhou Institute of Geochemistry, Chinese Academy of Sciences, Guangzhou, China, [2]CAS Center for Excellence in Tibetan Plateau Earth Science, Beijing, China, [3]School of Geosciences, Division of Geology and Geophysics, University of Sydney, Sydney, New South Wales, Australia, [4]Institute of Earth Sciences, Academia Sinica, Taipei, Taiwan, [5]Department of Geosciences, National Taiwan University, Taipei, Taiwan, [6]Guangxi Key Laboratory of Hidden Metallic Ore Deposits Exploration, College of Earth Sciences, Guilin University of Technology, Guilin, China, [7]Key laboratory of Mineralogy and Metallogeny, Guangzhou Institute of Geochemistry, Chinese Academy of Sciences, Guangzhou, China

Abstract Genesis of adakites in arc and nonarc tectonic settings plays an important role in magmatic processes and material recycling along convergent margins. However, little is known about characteristics of pristine adakitic melts due to late stage magma evolutionary processes that dilute or obscure primary melt features, and thus, the genesis of adakites remains controversial. Here we present a detailed analysis of amphibole composition from Early Permian Awulale postcollisional adakitic diorite and granodiorite porphyries in the core of Tianshan Orogen, the central Asian orogenic belt. Two distinct populations of amphiboles, with markedly different aluminum contents, are observed in the adakitic rocks. These are (1) high-Al amphiboles, crystallizing as an early mineral phase at about 1 GPa, and (2) low-Al amphiboles, as a late mineral phase at 220–400 MPa, estimated on the basis of experimental phase equilibria data. Trace element modeling indicates that melts in equilibrium with the high-pressure amphiboles are of adakitic composition, suggesting that the Awulale pristine magmas already had an adakitic nature before the amphibole crystallization. This is consistent with the mafic lower crustal melting model, rather than a high-pressure basaltic melt fractionation, for adakite petrogenesis. Our results lend new insights into how amphibole composition can be used to constrain the geochemical characteristics of pristine adakitic magmas.

Plain Language Summary Genesis of adakites in arc and nonarc tectonic settings plays an important role in magmatic processes and material recycling along convergent margins. In addition to the original slab melting scenario, petrogenesis of adakites remains highly controversial with two principal competing models. One involves melting of thickened mafic lower crust. The other involves high-pressure (e.g., ~1.0–1.5 GPa) crystal fractionation of normal basaltic arc magmas. Here we present a detailed analysis of amphibole composition from postcollisional adakites in the core of Tianshan Orogen. Two distinct populations of amphibolesare observed in the adakitic rocks. These are (1) high-Al amphiboles, crystallizing as an early mineral phase at about 1 GPa, and (2) low-Al amphiboles, as a late mineral phase at 220–400 MPa, estimated on the basis of experimental phase equilibria data. Trace element modeling indicates that melts in equilibrium with the high-pressure amphiboles are of adakitic composition, suggesting that the Awulale pristine magmas already had an adakitic nature before the amphibole crystallization. This is consistent with the mafic lower crustal melting model, rather than a high-pressure basaltic melt fractionation, for adakite petrogenesis. Our results lend new insights from amphibole compositions that can be used to constrain the geochemical characteristics of pristine adakitic magmas.

1. Introduction

Adakite was originally named by *Defant and Drummond* [1990] after the "type locality" Adak Island in the Aleutian arc where the first example was reported for some intermediate-acid volcanic rocks as the product of melting subducted oceanic slab [*Kay*, 1978]. The rock is characterized by high Al_2O_3 (>15 wt %), Sr (>400 ppm), low-Y (<18 ppm), and heavy rare earth elements (HREEs, Yb < 1.9 ppm), coupled with high Sr/Y (>40), strikingly fractionated REE (La/Yb > 20), and a lack of obvious Eu anomalies [*Castillo*, 2006, 2012; *Defant and Drummond*, 1990]. The importance of adakites stems from the fact that (i) many of them are found in settings associated with subduction of young (≤25 Ma) hence hot oceanic lithosphere, leading

to the proposal that they formed from melting of the basaltic crust of subducted slabs in the garnet amphibolite or eclogite facies [*Defant and Drummond*, 1990; *Kay*, 1978; *Martin et al*., 2005]; (ii) they are geochemically similar to the Archean trondhjemite-tonalite-granite suite and as such may be key to understanding crustal generation during the Archean; and (iii) many porphyry-type deposits worldwide are associated with magmas showing some adakitic geochemical features [*Richards and Kerrich*, 2007; *Sun et al*., 2012], and thus, adakites supply most copper and significant gold to our economy.

The genesis of adakites has attracted increasing interest and debate during the last two decades [see *Castillo*, 2012, and references therein]. In the original adakites genetic model, the magmas are derived from the melting of subducted oceanic crust under pressure-temperature (*P-T*) conditions where garnet is stable and plagioclase is not. They are characterized by normal mid-oceanic ridge basalt (N-MORB)-like depleted isotopic compositions, along with high MgO, Ni, and Cr contents that suggest interaction between slab melts and subarc mantle peridotites [*Defant and Drummond*, 1990; *Kay*, 1978]. The slab melting process has been supported by the results of a wide range of high-pressure melting experiments and field evidence consisting of adakite-like glass inclusions in arc peridotites, and adakite-like veins in obducted oceanic slab and xenoliths [*Castillo*, 2012, and references therein]. However, slab melting is only achieved at higher temperature (~1000°C at 1.5 GPa) conditions when a young (i.e., hot) oceanic plate subducts with a hot geothermal gradient [*Peacock et al*., 1994]. Thus, slab melting only occurs under specific geodynamic conditions in modern subduction zones, such as the opening of a slab tear [*Ribeiro et al*., 2016], ridge subduction [*Tang et al*., 2010], and plume-slab interaction [*Lee and Lim*, 2014]. The transitory nature of conditions that favor slab melting are consistent with the observation that slab-derived adakite magmas are volumetrically insignificant compared with normal arc magmas [*Hoernle et al*., 2008].

In addition to the original slab melting scenario, petrogenesis of adakites, which occurs not only in modern subduction zones but also in ancient orogenic belts, remains highly controversial with two principal competing models. One involves melting of thickened mafic lower crust in the garnet stability field with little or no contribution of melts from the plagioclase stability field [*Atherton and Petford*, 1993; *Chung et al*., 2003; *Wang et al*., 2005]. The other involves high-pressure (e.g., ~1.0–1.5 GPa) crystal fractionation of normal basaltic arc magmas [*Castillo*, 2006; *Macpherson et al*., 2006; *Prouteau and Scaillet*, 2003; *Richards and Kerrich*, 2007]. Adakitic magmas generated by either of these processes are commonly characterized by enriched isotopic signatures compared with N-MORB, along with distinct low MgO, Ni, and Cr contents, because they experience no interaction with mantle peridotites [*Atherton and Petford*, 1993; *Castillo*, 2006; *Chung et al*., 2003; *Wang et al*., 2005]. It is difficult to distinguish between these two models solely on the basis of geochemical data due to late stage magma evolution that dilutes primary melts features. Thus, pristine adakitic melts provide fresh and illuminating information for studies of adakite petrogenesis.

Amphiboles are the first mineral phase to crystallize in most adakitic magmas [*Prouteau and Scaillet*, 2003]. They contain abundant information on pristine magma compositions and magma crystallization depths [*Prouteau and Scaillet*, 2003; *Scaillet and Evans*, 1999]. Thus, amphibole compositions can be used to constrain the nature of associated equilibrium melts and their storage depths. For example, amphibole has been recently studied in order to estimate magma storage depths and the composition of the host melts for subduction zones adakites by *Ribeiro et al*. [2016]. They argued that slab melting is not necessarily required to produce adakites in hot subduction zones.

In this study, we identify two distinct groups of amphiboles in the Early Permian postcollisional adakitic plutons from the west Awulale Mountains in the core of the Tianshan Orogen (Figure 1). The amphiboles are used to constrain magma storage depths and the compositional characteristic of the melts in equilibrium with the crystals. Our results show that the melts in equilibrium with the high-pressure amphiboles from the Awulale adakitic rocks already had adakitic characteristics prior to amphibole formation. In contrast, the melts in equilibrium with low-pressure amphiboles did not display adakitic geochemical features. The data offer critical new clues to the long lasting controversy regarding adakite petrogenesis.

2. Early Permian Adakitic Rocks in Tianshan Orogen

2.1. Geological Background

As "the backbone of Central Asia," the Tianshan Orogen is a major component of the southwestern Central Asian Orogenic Belt (Figures 1a and 1b). It reflects Paleozoic subduction accretion involving the

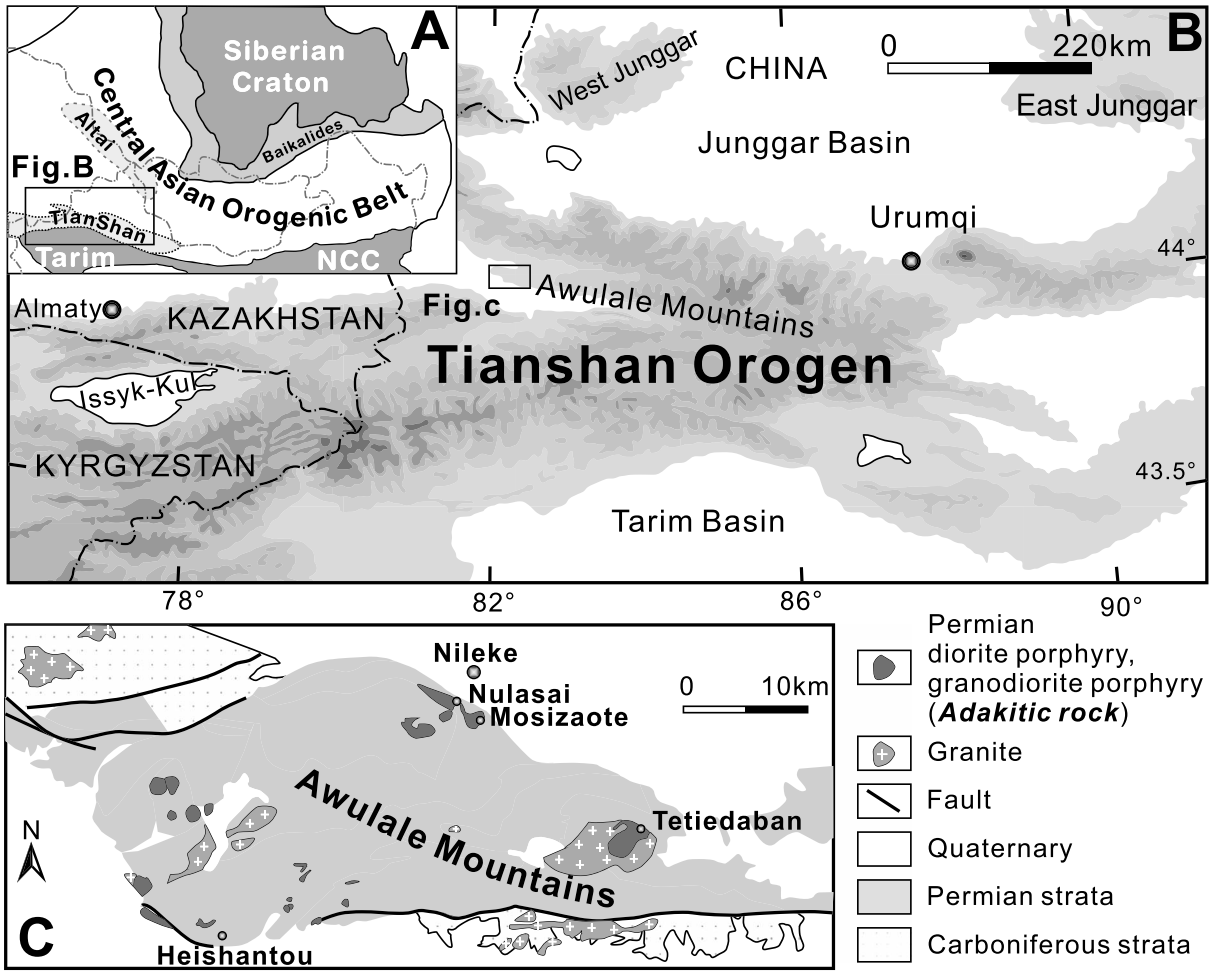

Figure 1. (a) A simplified geological map of the CAOB (modified from *Jahn et al.* [2000]), NCC: North China Craton. (b) Topographic map of the Tianshan Orogen, showing the locations of the Awulale Mountains in the core of the Tianshan [after *Han et al.*, 2010]. (c) Geological map of the west part of the Awulale Mountains, showing locations of adakitic intrusions [*Zhao et al.*, 2008].

Paleo-Asian Ocean, terminal continental collision at the end of the Carboniferous, and a transition to a postcollisional setting during the Early Permian, evidenced by the presence of ~300 Ma oldest stitching granitic plutons and Permian postcollisional plutons and molasse sedimentation in the Tianshan Orogen [*Gao et al.*, 2011; *Han et al.*, 2011].

The Early Permian adakitic rocks in the western Awulale Mountains consist of numerous small diorite porphyry and granodiorite porphyry plutons and dikes (Figure 1c). They intruded into the Early Permian volcanic-sedimentary strata at 272 ± 3 Ma (Figure S1 and Table S1).

2.2. Petrology

All the adakitic rocks show porphyritic textures (Figure 2). The diorite porphyries are crystal-rich rocks with ~40 vol % phenocrysts. The phenocrysts are (in the order of relative abundance) plagioclase, amphibole, quartz, K-feldspar, and biotite with subhedral to euhedral shapes. Amphibole crystals generally show oscillatory zonation. Plagioclase crystals may occasionally partly or totally enclose some amphibole grains, consisting with that amphiboles crystallization prior to, or in equilibrium with plagioclase. The groundmass exhibits hyalocrystalline pilotaxitic, and micrograined textures defined mainly by plagioclase with less quartz and K-feldspar. The granodiorite porphyries are crystal-poor rocks with ~20 vol % phenocrysts that include plagioclase, amphibole, biotite, quartz, and K-feldspar with euhedral shapes. Most amphibole crystals show no compositional zoning (Figure 2). Magnetite, ilmenite, apatite, and zircon are the main accessory minerals in both types of rocks.

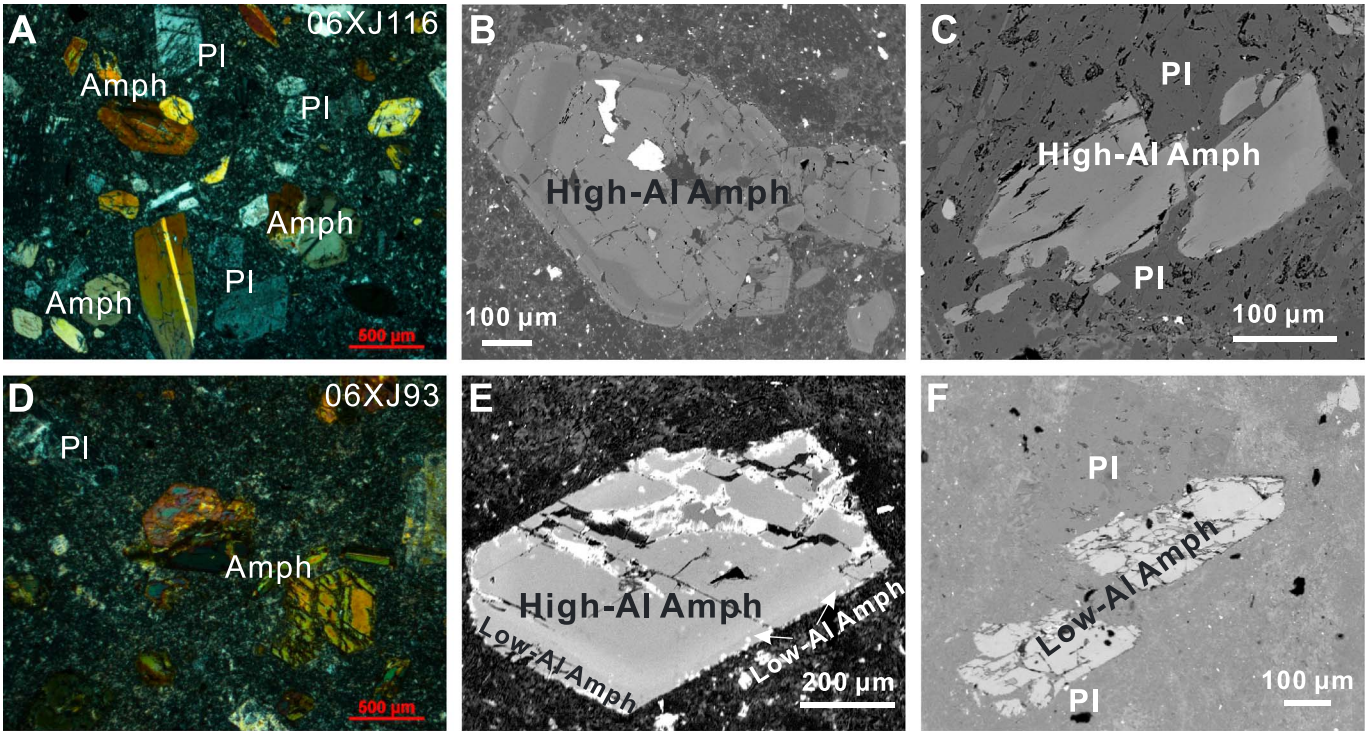

Figure 2. Representative cross-polarized light photomicrographs showing typical (a) diorite porphyry and (d) granodiorite porphyry with phenocrysts of plagioclase (pl) and amphibole (amph). Backscattered electron microscope images of amphibole phenocrysts in (b, c) diorite porphyry and (e, f) granodiorite porphyry.

3. Minerals Analytical Methods

Major element analysis and backscattered electron (BSE) imaging of minerals were carried out using a JEOL JXA-8230 electron microprobe Superprobe at the College of Earth Sciences, Guilin University of Technology. An accelerating voltage of 15 kV, a specimen current of 3.0×10^{-8} A, and a beam size of 1–2 μm were employed. The data reduction was carried out using ZAF correction.

In situ mineral trace element analysis was carried out by laser ablation (LA)-ICP-MS technique using an Agilent 7500a ICP-MS system coupled with a GeoLas193 nm ArF-excimer laser sampler at State Key Laboratory of Isotope Geochemistry, Guangzhou Institute of Geochemistry, Chinese Academy of Sciences (GIG-CAS). Both double-volume sampling cell and Squid pulse smoothing device were used to improve the data quality. A spot size of 51 μm and repetition rate of 6 Hz were applied during the analysis. Calibration was carried out externally using National Institute of Standards and Technology SRM 612 with Ca as an internal standard to correct for any drift. Repeated analyses of the USGS rock standards (BHVO-2G and BCR-2G) indicate precision and accuracy both better than 4% for most elements analyzed. After the analytical procedures, quantitative calibration for trace element abundances was performed using ICPMSDataCal [*Liu et al*., 2008]. Analytical details have been given by *Tu et al*. [2011].

4. Results

Analytical methods of zircon U-Pb dating, Hf isotope composition, and whole-rock element and Nd isotope composition are given in Text S1 in the supporting information. Zircon U-Pb geochronology is described in the Text S2. Zircon concordia diagram is presented in Figure S1.

4.1. Geochemistry of the Early Permian Awulale Adakitic Rocks

The Awulale rocks have a wide range of SiO_2 contents, ranging from 60.4 to 71.9 wt %, and low MgO contents ranging from 0.4 to 2.7 wt %. They are medium-K to high-K calc-alkaline with K_2O contents ranging from 1.6 to 5.7 wt % (Figure 3). These rocks are characterized by high Sr (303–1633 ppm) but low Y (2.4–7.0 ppm) and Yb (0.24–0.65 ppm) contents, with elevated Sr/Y (51–336) and highly fractionated rare earth element (REE)

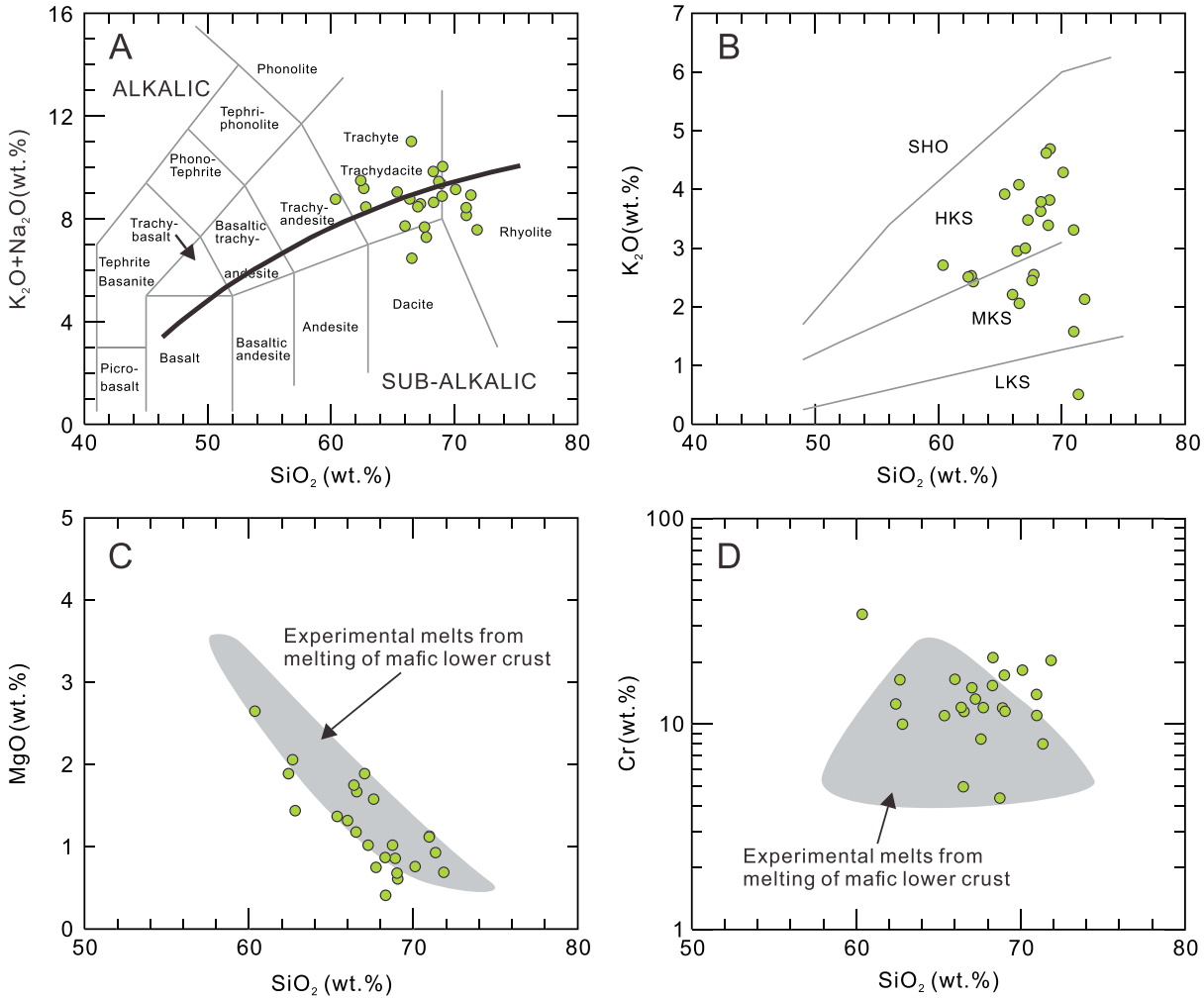

Figure 3. (a) Total alkalis versus SiO_2 diagram [*Le Maitre*, 2002]; the dashed line separating alkaline series from subalkaline series is from *Irvine and Baragar* [1971]. (b) K_2O versus SiO_2 diagram [*Peccerillo and Taylor*, 1976]; LKS, MKS, HKS, and SHO are low-K tholeiite series, medium-K calc-alkaline series, high-K calc-alkaline series, and shoshonitic series, respectively. (c) MgO versus SiO_2 diagram. (d) Cr versus SiO_2 diagram. The experimental melts of melting of mafic lower crust (1.0–1.5 GPa) [*Qian and Hermann*, 2013] are shown for comparison.

patterns with high $(La/Yb)_N$ ratios (14–53). Most samples have negligible to positive Eu anomalies with Eu/Eu* = 0.98–1.45 (Figure 4). They show typical adakitic geochemical characteristics, the typical Cenozoic adakites derived by partial melting of thickened lower crust from South Tibet (Figure 4). They have juvenile isotope compositions with positive whole rock $\varepsilon_{Nd}(t)$ (+1.0 to +3.4) and zircon $\varepsilon_{Hf}(t)$ (+5.4 to +11.2) values (Tables S2 and S3).

4.2. Amphibole Zoning and Composition

Major and trace elements data are presented in Tables S4 and S5, respectively. Amphibole compositions were filtered to retain major oxide compositions with oxide sums of 98 ± 2 wt %. Two distinct populations of amphiboles, distinguished by their aluminum contents, were observed in the adakitic rocks (Figure 5 and Table S4). High-Al amphiboles (Al_2O_3 = 11.1–15.4 wt %) occur as the only amphibole phase in diorite porphyries. Faint concentric growth zonation is a commonly observed zoning pattern in the amphibole crystals (Figure 6). These crystals consist of dark or bright cores with oscillatory zoned from core to rim. Brighter zones are richer in Al than the dark regions. In addition, some amphibole crystals are simple zoned, and it occurs in two subtypes, which can be distinguished by their compositional zones from core to rim. Subtype 1 zoning is characterized by dark cores with thin brighter rims. Subtype 2 zoning crystals have bright cores that are typically rounded, which are surrounded by dark rims. All crystals show compositional variation at the high-Al

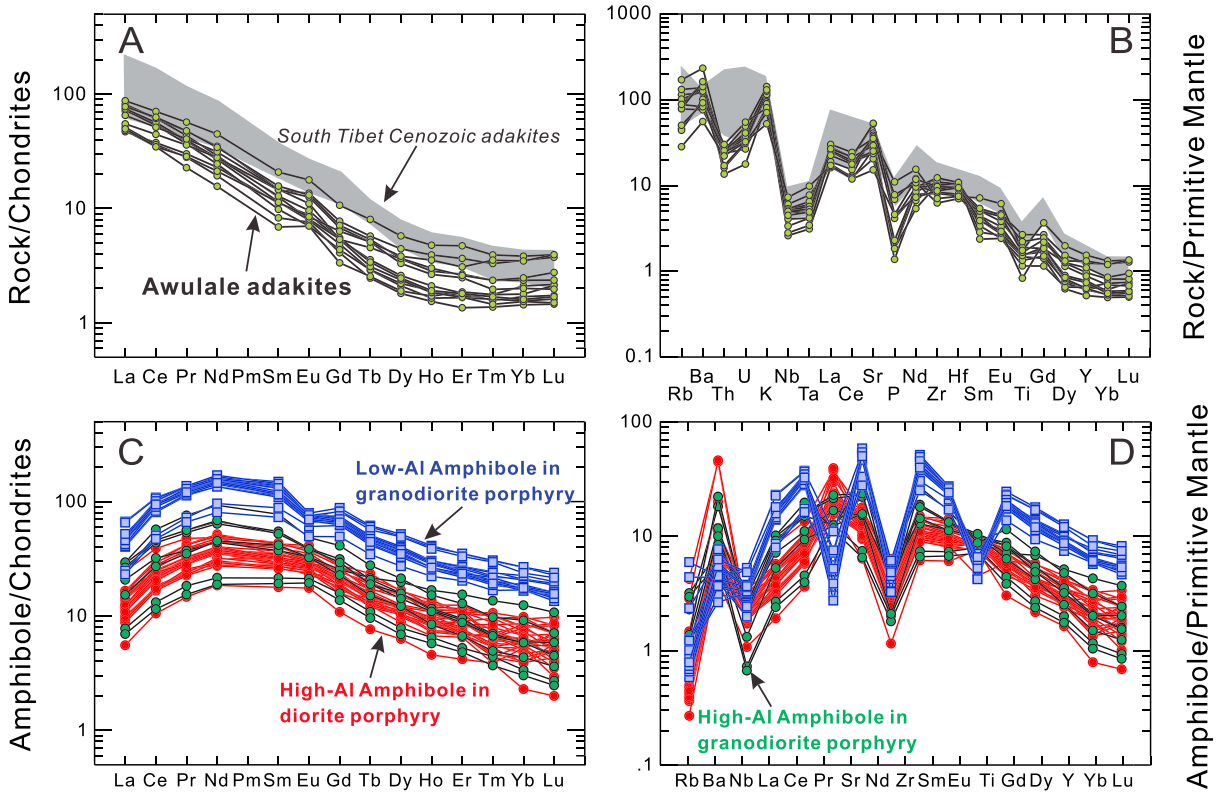

Figure 4. (a) Chondrite-normalized rare earth element patterns and (b) primitive mantle-normalized trace element patterns for the Awulale adakitic rocks. (c) Chondrite-normalized rare earth element patterns and (d) primitive mantle-normalized trace element patterns for the amphiboles from the Awulale adakitic rocks. In the Figures 4a and 4b, the fields of the typical Cenozoic adakites derived by partial melting of thickened lower crust from South Tibet are shown for comparison [*Chung et al.*, 2003]. Chondrite and primitive mantle normalizing values are from *Sun and McDonough* [1989].

level (Figure 6). They are mainly magnesiohastingsite with minor tschermakite [*Leake et al.*, 1997], with $(Na + K)_A$ ranging from 0.30 to 0.76 and Mg number [molar $Mg/(Mg + Fe^{tot})$] from 0.57 to 0.80 (Figure 5).

In contrast, granodiorite porphyries contain both high-Al ($Al_2O_3 = 11.1–13.2$ wt %) and low-Al ($Al_2O_3 = 5.5–10.8$ wt %) amphiboles. These amphiboles show a variety of zoning patterns (Figures 2 and 7). Some of the amphiboles display weak or no apparent zonation in BSE images and have uniform low Al_2O_3 contents from core to rim. A second amphibole zoning style in the granodiorite porphyries is characterized by a simple abrupt shift in Al at the core-rim boundary. Still other crystals have high Al_2O_3 (brighter) cores with thin low Al_2O_3 (darker) rims or show reversed zoning with low Al_2O_3 cores and high Al_2O_3 rims (Figure 7). Oscillatory zonation was also observed in the amphibole crystals with thin Al spikes at their mantles. The high-Al amphiboles are tschermakite and magnesiohastingsite, with $(Na + K)_A$ from 0.3 to 0.6 and Mg number from 0.57 to 0.74. Low-Al amphiboles are principally magnesiohornblende, with low $(Na + K)_A$ (0.05–0.5) and Mg number (0.58–0.72) (Figure 5).

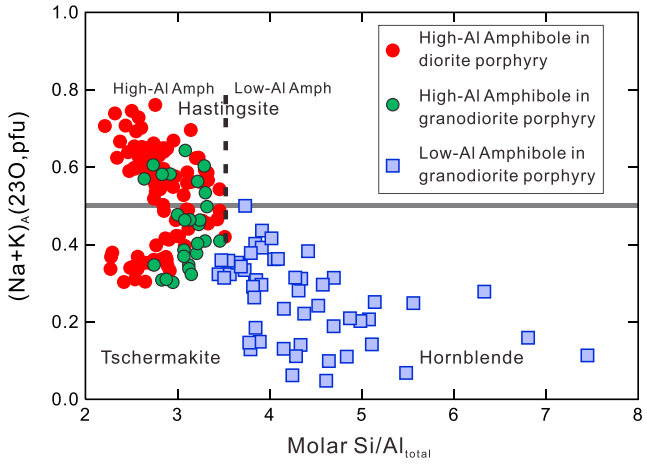

Figure 5. Compositional variations of amphiboles in the Awulale adakitic rocks on the diagram of molar Si/Al_{tot} versus $(Na + K)_A$ per formula unit (pfu).

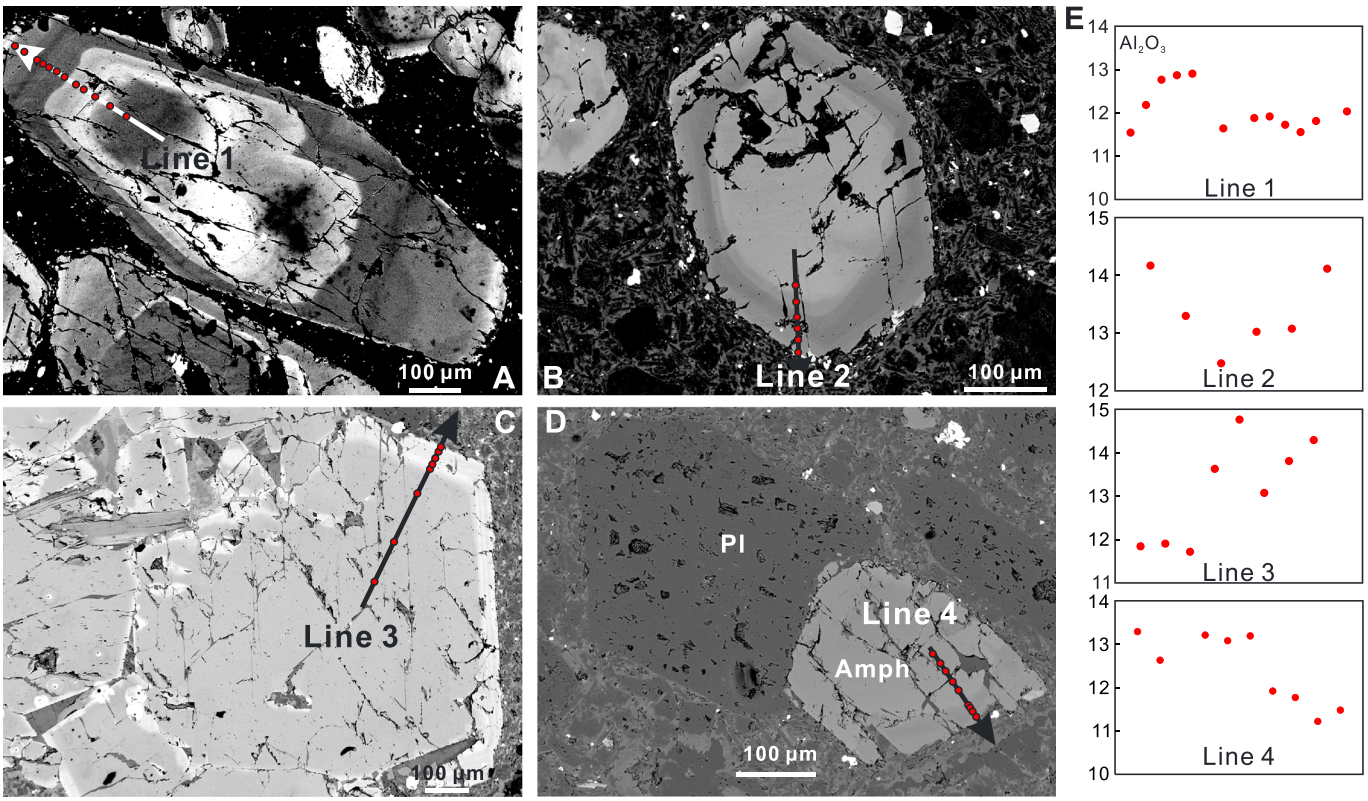

Figure 6. (a–d) BSE images showing the zoning patterns and textures of amphiboles in the diorite porphyry. (e) Compositional profiles of Al_2O_3 of amphiboles are indicated by arrows. BSE image displaying oscillatory zoned an amphibole phenocryst (Figures 6a and 6b). BSE image showing a high-Al core with thin low-Al rim for an amphibole phenocryst (Figure 6c). BSE image showing the coexist of amphibole and plagioclase phenocrysts, and the amphibole has a low-Al core with high-Al rim (Figure 6d).

All high-Al amphiboles in diorite and granodiorite porphyries reveal convex upward chondrite-normalized patterns, with Nd maxima at about 4 times chondrite. The low-Al amphiboles in granodiorite porphyries have higher trace elements contents that are 3–5 times greater than those of high-Al amphiboles (Figure 4 and Table S5). The REE patterns of the low-Al amphiboles are similar with high-Al amphiboles, but with distinct negative Eu anomalies. The high-Al amphiboles in both the diorite and granodiorite porphyries have identical geochemical compositions, which are characterized by strongly positive Sr anomalies but no Ti anomalies on primitive mantle-normalized trace element diagrams. Low-Al amphiboles show both strongly negative Sr and Ti anomalies (Figure 4). The negative Sr and Eu anomalies of the low-Al amphiboles indicate their crystallization after plagioclase, which is consistent with the presence of plagioclase inclusions in amphiboles of the granodiorite porphyries.

5. Discussion

5.1. Magma Storage Depths

Empirical and experimental studies have indicated that amphibole compositions can be effectively used to estimate the pressure and temperature conditions during crystallization of calc-alkaline igneous rocks [*Anderson et al.*, 2008; *Anderson and Smith*, 1995; *Blundy and Holland*, 1990; *Hammarstrom and Zen*, 1986; *Holland and Blundy*, 1994; *Johnson and Rutherford*, 1989; *Putirka*, 2016; *Ridolfi et al.*, 2010; *Schmidt*, 1992]. Here we constrain magma *P-T* conditions for the Awulale adakitic rocks first based primarily on phase equilibrium experimental data established for the Pinatubo dacite [*Prouteau and Scaillet*, 2003; *Scaillet and Evans*, 1999] (Figure 8) that are consistent with the observed order of mineral crystallization and conventional mineral geobarometers, and then application of different amphibole thermobarometric techniques.

Variations in amphibole Al_{tot}, Na + K, and $Mg^{\#}$ contents are associated with pressure and temperature, as indicated by the amphibole experiments [*Alonso-Perez et al.*, 2009; *Prouteau and Scaillet*, 2003; *Samaniego et al.*,

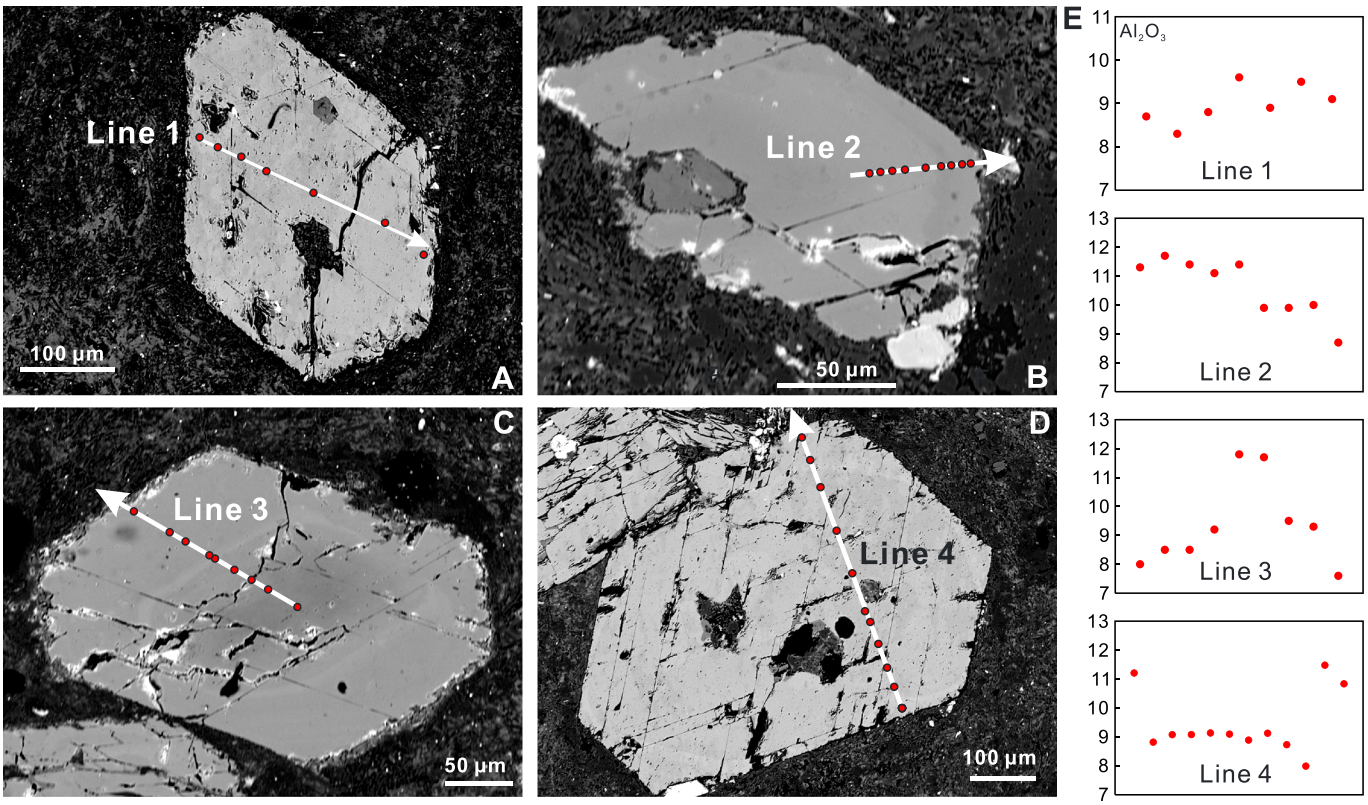

Figure 7. (a–d) BSE images showing the zoning patterns and textures of amphiboles in the granodiorite porphyry. (e) Compositional profiles of Al_2O_3 of amphiboles are indicated by arrows.

2010; *Scaillet and Evans*, 1999]. The crystallizations and melting experiments have verified that the pressures estimated with the experimental and Al-in-hornblende geobarometers approximately agree at a wide range of the calibration conditions where pressures and temperatures range from 220 to 1200 MPa and 700 to 1000°C, respectively [*Samaniego et al*., 2010]. Consequently, the experimental amphibole compositions can provide valuable geobarometric constraints.

To constrain the magma storage depths of the Early Permian Awulale adakitic rocks in the core of the Tianshan Orogen, we use the amphibole composition of the adakitic rocks compared with the compositions of experimental amphibole on the Al_{tot} versus Na + K and $Mg^{\#}$ diagrams. *Ribeiro et al*. [2016] and *Samaniego et al*. [2010] adopted a similar approach to assess the petrogenesis of adakites from the Philippines, Baja California, and Ecuador. Covariations in Al_T, Na + K, and $Mg^{\#}$ of the amphiboles from the Awulale adakitic rocks indicate that they are suitable for determining pressure conditions during crystallization. The high-Al amphiboles in both the diorite and granodiorite porphyries are characterized by high Na + K contents and Mg numbers in addition to high Al, and cluster in the 960 MPa field. In contrast, the low-Al amphiboles have lower contents in Al and Na + K and Mg numbers, and most of them fall in the 220 and 400 MPa fields on the Al versus Na + K and Mg number diagrams. Although the low-Al amphiboles do not strictly overlap with the fields of experimental Pinatubo amphibole on the Al versus Na + K diagram, the overall lower Al contents are indicative of low pressure of crystallization in the 220 and 400 MPa range.

Several studies have shown that the Al-tschermak substitution is susceptible to variations in pressure, whereas the plagioclase and edenite exchanges are temperature dependent [*Bachmann and Dungan*, 2002; *Blundy and Holland*, 1990]. The Ti-Tschermak exchange may reflect changes in pressure, water activity, and temperature, or any combination of these [*Adam et al*., 2007; *Bachmann and Dungan*, 2002; *Ernst and Liu*, 1998]. Amphibole compositional variations observed in the Awulale adakitic rocks can be explained by these exchange mechanisms, which relate to changes in pressure and temperature (Figure S2). Within the data set, there are good positive correlations of Al_{IV} with Al_{VI} (despite some scatter) and a positive

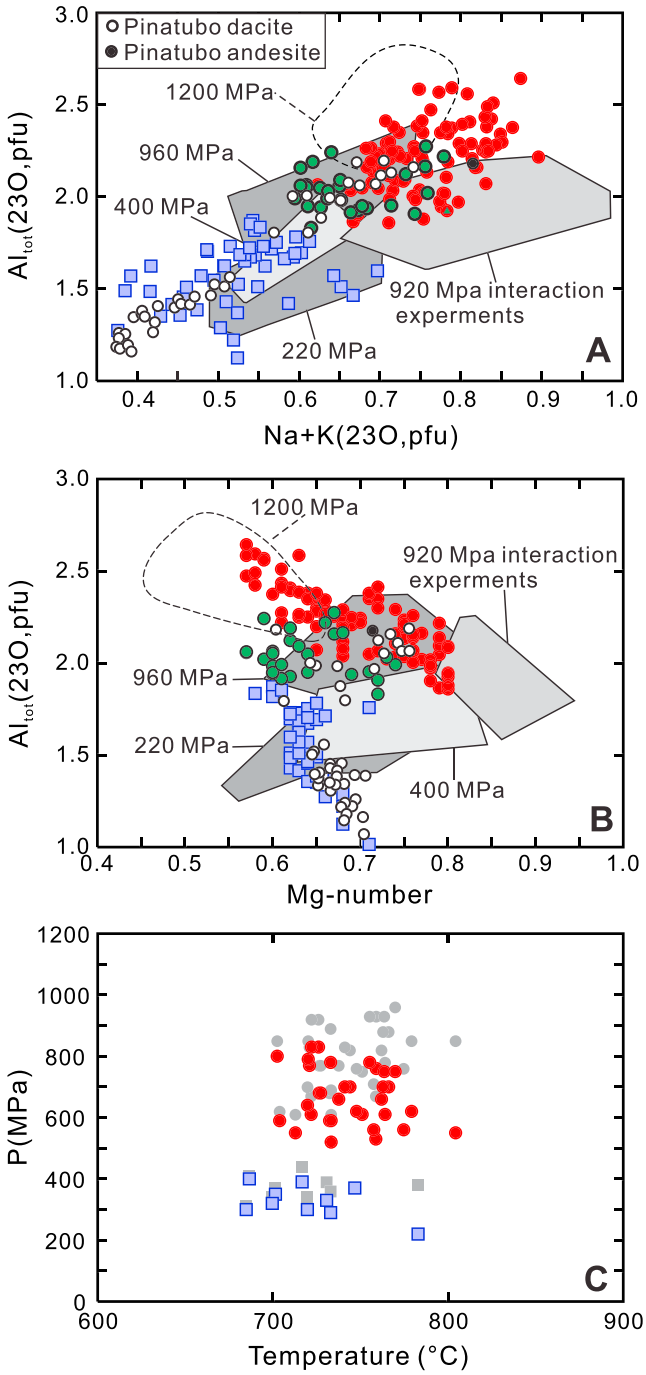

Figure 8. (a, b) High-Al (HP) and low-Al (HP) amphiboles from the Awulale adakitic rocks, compared with field for natural amphiboles in the 1991 Pinatubo dacite and andesite [*Bernard et al.*, 1991, 1996], and experimental amphiboles produced in the dacite system at 220 MPa [*Scaillet and Evans*, 1999], 400 and 960 MPa [*Prouteau and Scaillet*, 2003], and andesite at 1200 MPa [*Alonso-Perez et al.*, 2009]. (c) Estimated pressures and temperatures for Awulale adakitic rocks based on the Al-in-hornblende calibration of *Anderson and Smith* [1995] and temperatures from the hornblende-plagioclase calibration of *Holland and Blundy* [1994]. Gray symbols correspond to pressure estimates based on the Al-in-hornblende calibration of *Schmidt* [1992].

correlation of Al_{VI} with Al_T (not shown), which are consistent with Al-tschermak exchange and hence variations in the pressure conditions. In addition, the amphibole Al_{IV} versus $Mg^{\#}$ interrelationships provide a better means to determine which parameters are responsible for the observed compositional variations [*Kiss et al.*, 2014]. Positive Al_{IV}-$Mg^{\#}$ trends in amphiboles reflect magma mixing where the high-Al amphiboles formed after mafic replenishment into a silicic capture zone. In these cases the high-Al amphiboles do not indicate deeper magma storage depths [*Kiss et al.*, 2014]. Importantly, such high-Al amphiboles form as a second generation after the mafic magma input and yield the same pressure results as low-Al amphiboles, based on Al-in-amphibole barometry [*Anderson and Smith*, 1995; *Schmidt*, 1992]. In the Awulale adakitic rocks, however, there is no positive relationship between Al_{IV} and $Mg^{\#}$ in the amphiboles (Figure S2) and the issue is not a concern.

Petrographic observations suggest that all amphiboles could crystallize along with the mineral assemblage that is required for the amphibole thermobarometric calculation (quartz + alkali feldspar + plagioclase + biotite + Fe-Ti oxide + titanite; see section 2.2) [*Anderson and Smith*, 1995]. Magma crystallization pressure and temperature were estimated through Al-in-amphibole barometers of *Anderson and Smith* [1995], at temperatures obtained with the *Holland and Blundy* [1994] hornblende-plagioclase thermometer (reaction edenite + albite = richterite + anorthite), using the spreadsheet published by *Anderson et al.* [2008] (RiMG069_Ch04_hbld_plag_thermojla.xls spreadsheet). We select the hornblende-plagioclase pairs, and only those analyses on phenocryst rims were utilized for calculation. Pressures were also calculated by

the temperature-independent geobarometer of *Schmidt* [1992] and were compared with results obtained from the calibration of *Anderson and Smith* [1995]. Results obtained with both procedures are plotted in Figure 8 and listed in Table S6.

The amphibole-plagioclase thermometry yields $T_{am\text{-}plag} = 720 \pm 28°C$ for mineral pairs of low-Al amphibole in the granodiorite porphyries, which are close to $T_{am\text{-}plag} = 743 \pm 23°C$ for the high-Al amphibole in the diorite porphyry (Figure 8). In contrast, the Al_{tot} in amphibole barometry ($P_{Al\text{-}in\text{-}am}$) indicates that the two amphibole groups crystallized at very different pressures. Pressures obtained with the method of *Anderson and Smith* [1995] for the high-Al amphiboles range between 520 and 830 MPa, whereas the low-Al amphiboles yielded lower values between 220 and 400 MPa. The results of *Schmidt* [1992] yielded slightly higher pressure than the results of *Anderson and Smith* [1995] for both high-Al and low-Al amphiboles (610–960 MPa; 310–440 MPa). Different calibration approaches of the composition of experimental amphiboles and Al-in-hornblende geobarometers yielded similar results for the pressure, with only minor discrepancies in the results obtained between them (Figure 8).

From the above arguments, two populations of amphiboles are observed: high-pressure and low-pressure generations corresponding to approximately 1 GPa and 220–400 MPa, respectively. Thus, amphiboles from the Awulale adakitic rocks crystallized in two storage zones: one localized in the lower crust (30–35 km) and the other near the middle-upper crust transition zone (7–15 km) (Figure 8).

5.2. Melt in Equilibrium With Amphiboles

The use of appropriate partition coefficients is required to ensure that the calculated equilibrium melts reliably reflect the composition of the parental magmas. The partition coefficients, however, are sensitive to changes in many parameters, such as melt composition, pressure, temperature, and redox state [*Tiepolo et al*., 2007]. The REEs, Sr and Y, were the key elements used to calculate the melts in equilibrium with the amphibole of the Awulale adakitic rocks. The trace element concentrations of the melts in equilibrium with the amphibole phenocrysts were calculated using andesite and dacite partition coefficients for the high- and low-pressure amphiboles [*Chambefort et al*., 2013; *Sisson*, 1994], respectively, but they vary insignificantly. In addition, the equilibrium melts, calculated using the hornblende-adakite partition coefficients of *Hidalgo et al*. [2007] recommended by *Ribeiro et al*. [2016], show insignificant differences with our results using the above partition coefficients. Furthermore, the calculated equilibrium melts show similar REE patterns to their adakite hosts (Figure 9), indicating that the partition coefficients are appropriate for determining the parental melt compositions.

Melts in equilibrium with the high-pressure amphibole are characterized by marked REE fractionation and low heavy REE concentrations typical of adakites with high La/Yb_N ratios (15–35) and low Yb (6–12 ppm) relative to the low-pressure amphiboles. Furthermore, the melts in equilibrium with the high-pressure amphibole are characterized by higher Sr/Y ratios (60–220) and lower Y (6–14 ppm) relative to those of the low-pressure amphiboles (2–9 and 23–36 ppm), respectively. They yield REE compositions similar to the whole-rock range of the Awulale diorite porphyries. However, melts in equilibrium with the low-pressure amphiboles yield REE compositions greater than the observed whole-rock compositions without adakitic geochemical features (Figure 9).

5.3. Evaluating the Three Competing Models

It is unlikely that the Awulale adakitic rocks formed by partial melting of a subducted oceanic slab, simply because in the Early Permian the Tianshan Orogen had evolved to a postcollisional setting [*Gao et al*., 2011; *Han et al*., 2011]. In addition, the adakite's slightly enriched Sr-Nd isotope compositions (Tables S2 and S3) and low MgO (<2.7 wt %) and Cr (<35 ppm) contents (Figure 3) do not support a slab melting origin [*Defant and Drummond*, 1990; *Kay*, 1978].

To discriminate between high-pressure fractionation of basaltic melt and partial melting of lower mafic crust in the garnet stability field, we consider what the key differences would be between adakitic magmas generated by each mechanism. In the high-pressure fractionation model, the original hydrous arc basalts, derived from the metasomatized mantle wedge, pond in a lower crust deep reservoir [*Macpherson et al*., 2006]. They began to cool and crystallize a high-pressure mineral assemblage, including garnet and amphibole [*Coldwell et al*., 2011; *Macpherson et al*., 2006; *Prouteau and Scaillet*, 2003]. Fractionation of both garnet

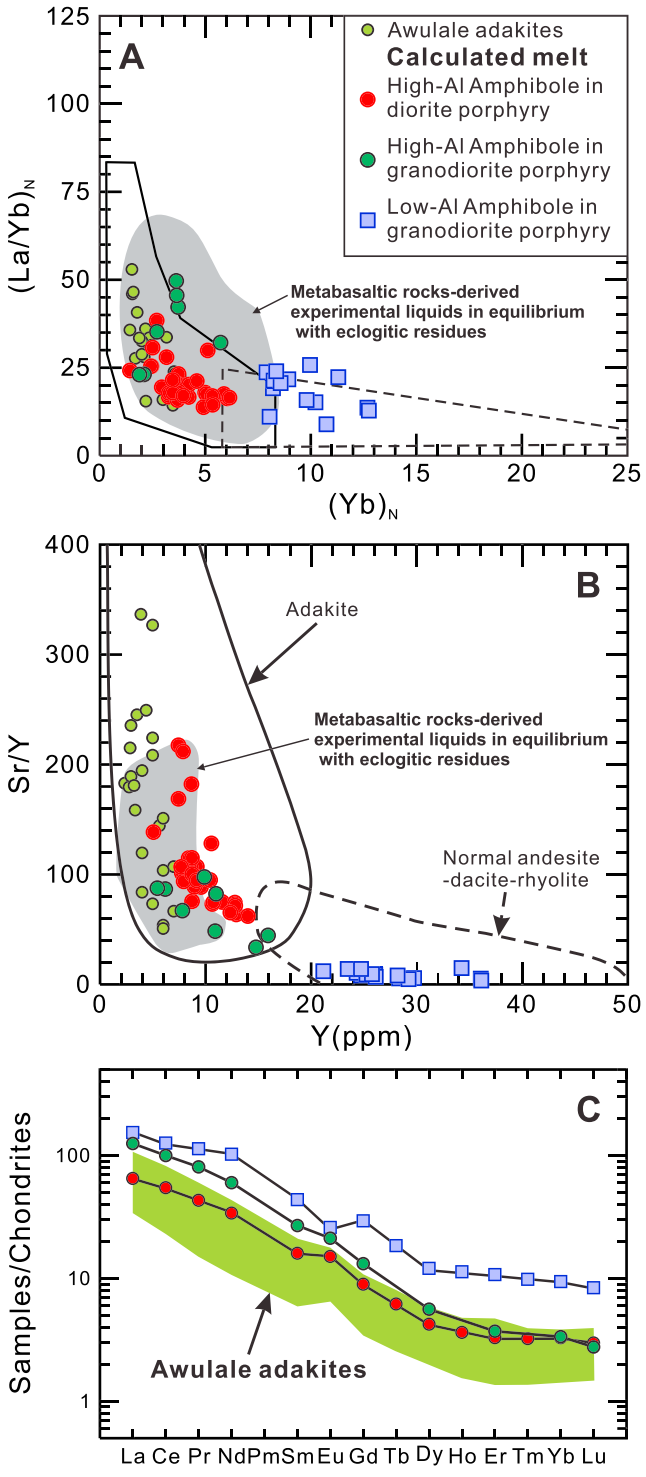

Figure 9. (a, b) $(La/Yb)_N$ versus Yb_N and Sr/Y versus Y diagrams [*Defant and Drummond*, 1990]. (c) Chondrite-normalized REE patterns for the two distinct populations of amphiboles compared with Awulale adakitic rocks. The calculated melts in equilibrium with HP and LP amphiboles are shown for comparison. The eclogite experimental melts (2.0–4.0 GPa) [*Rapp et al.*, 2003] are shown for comparison. Data are normalized to the Chondrite values of *Sun and McDonough* [1989].

and amphibole can induce significant HREE and Y depletions in residual melt and generate adakitic magmas [*Davidson et al.*, 2007; *Macpherson et al.*, 2006]. The resultant adakitic magmas would then ascend to a shallow reservoir, where a low-pressure phenocryst assemblage crystallizes, that is dominated by amphibole and plagioclase [*Coldwell et al.*, 2011; *Macpherson et al.*, 2006; *Prouteau and Scaillet*, 2003].

In the lower mafic crust partial melting model, adakitic magmas can be produced directly by partial melting of lower crust, thickened by arc basalt underplating, in the garnet and amphibole stability fields but below the plagioclase stability field [*Atherton and Petford*, 1993; *Chung et al.*, 2003; *Kay et al.*, 2005; *Wang et al.*, 2005]. After that, the adakitic magmas migrate upward and pond in a shallow reservoir, where low-pressure minerals such as amphibole and plagioclase crystalize as in the former model.

In the high-pressure fractionation model, the melts in equilibrium with high-pressure amphiboles clearly have arc basalt compositions [*Macpherson et al.*, 2006]. In contrast, the high-pressure amphiboles are in equilibrium with adakitic magmas in the lower mafic crust melting model. The melts in equilibrium with low-pressure amphiboles in both models may have adakitic compositions or not, depending on the relative proportions of the fractionating amphibole and plagioclase phases [*Foley et al.*, 2013]. Following fractionation of an amphibole or amphibole-dominated mineral assemblage, the magma would retain its adakitc features. In contrast, fractionation of plagioclase or a plagioclase-dominated mineral assemblage can dramatically drive adakitic magmas into the normal

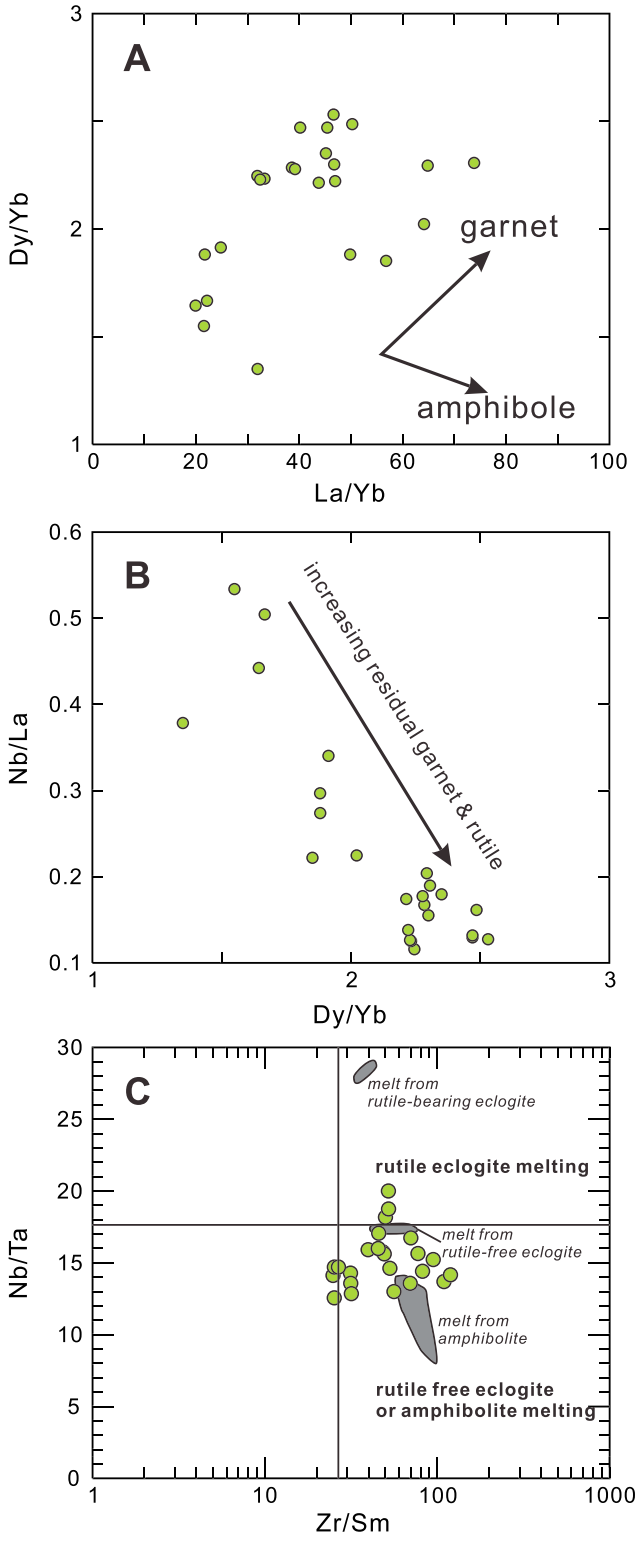

Figure 10. Trace element ratios of the Awulale adakitic rocks. (a) Dy/Yb versus La/Yb diagram; trend lines show garnet and amphibole fractionation. (b) Nb/La versus Dy/Yb diagram; variation trend with increasing residual garnet and rutile is from *Xiong et al.* [2011]. (c) Zr/Sm versus Nb/Ta [*Foley et al.*, 2002]. Nb/Ta versus Zr/Sm diagram for the Awulale adakitic rocks from the Tianshan Orogen. Shaded areas represent melt composition of experiments by *Foley et al.* [2002].

arc magma compositional field [*Sun et al.*, 2012].

5.4. Our New Approach: An Amphibole Perspective

Consequently, we argue that the melt compositions in equilibrium with the high-pressure amphiboles provide important constraints on adakite petrogenesis and discriminate between the two principal processes. For the Awulale adakitic rocks, the melts in equilibrium with the high-pressure amphiboles already had adakitic characteristics. Thus, our amphibole data are difficult to reconcile with a high-pressure fractionation model and lower mafic crust melting is suggested to be responsible for generation of the Awulale Early Permian adakitic rocks. The melts in equilibrium with the low-pressure amphiboles from the granodiorite porphyries do not show adakitic features. The result implies that while the magma bulk composition (liquid plus crystals) retained adakitic features, the remaining melt had evolved away from an adakite composition. This observation implies fractionation of a plagioclase-dominated mineral assemblage over amphibole at low pressures. The absence of low-pressure amphibole in the diorite porphyry probably reflects rapid cooling of a magma that was generated by lower mafic crust melting. The rapid cooling is further supported by the similar temperature ranges associated with the high- and low-pressure amphiboles in the adakites (Figure 8), which most probably was induced by convective removal of collision-thickened Tianshan lithosphere, and thus melting of the thickened lower crust to produce adakitic magma. In contrast, the granodiorite porphyries contain both high- and low-pressure amphiboles that show complex zoning (Figure 7).

This feature indicates that deeply sourced adakitic magmas were hybridized by more fractionated magma batches at shallow levels.

It is important to note that the high-pressure amphiboles crystallized at about 1 GPa, which does not represent the actual depth of mafic lower crust melting. The depth of partial melting required to form the Awulale adakitic rocks can provide a key reference for the estimation of the crustal thickness of the Tianshan Orogen during Early Permian. At the same time, whether residual rutile and garnet occurred in the source is the critical factor for constraining the pressure and depth of adakitic magma generation.

The positively correlated Dy/Yb and La/Yb ratios (Figure 10) for the Awulale adakitic rocks suggest a dominant role of garnet in the REE fractionation, indicating a melting depth to produce adakitic magmas of at least ~1.0 GPa for garnet to be stable, based on experimental results [*Green*, 1982]. Furthermore, the Nb/La ratio decreases with increasing La/Yb ratio, and Nb/La ratios (0.10–0.55) (Figure 10) are lower than the lower crust average of 0.6 [*Rudnick and Gao*, 2003]. These relationships indicate that variable proportions of both residual garnet and rutile were responsible for Nb/La variations and other features in the Awulale adakitic rocks. In addition, Nb/Ta ratios have been proven to be the most sensitive pressure proxy, because the two elements are hardly affected by fractionation of garnet and amphibole [*Xiong et al*., 2005]. Rutile is a necessary residual phase in eclogite residue and fractionates Nb from Ta and melts generated below such a depth would possess higher Nb/Ta ratios than those formed under low-pressure (rutile-free) condition (Figure 10). The relatively high Nb/Ta ratios (14–20), and low Nb and Ta abundances are similarly consistent with strong partitioning of these elements into rutile [*Foley et al*., 2000; *Klemme et al*., 2005; *Xiong et al*., 2005]. Therefore, melting depth would therefore have been greater than 50 km, given that rutile is stable at pressures higher than ~1.5 GPa [*Xiong et al*., 2005].

Collectively, the Awulale adakitic magmas were derived from melting of thickened mafic lower crust at ~1.5 GPa, indicating a crustal source dominated by rutile eclogite, and then crystalized high-pressure amphiboles at about 1 GPa. After that, the adakitic magma rose into middle-upper crust transition zone (7–15 km) where a plagioclase-dominated mineral assemblage with low-pressure amphiboles crystallized.

Besides establishing a lower mafic crust melting model, the high-pressure amphibole compositions can also provide important insights for slab-melting models. If the high-pressure amphiboles indicate "regular" arc compositions and low-pressure amphiboles in the same rocks define adakitic compositions similar to their host, then these final compositions are likely to be the product of crystal fractionation. Such evidence was employed by *Ribeiro et al*. [2016] to suggest a crystal fractionation origin for the compositions of adakatic rocks from the Philippines. If, however, the pristine adakitic magmas were generated by slab or deep crustal melting at high pressure, then the melt compositions in equilibrium with the high-pressure amphiboles should show adakitic characteristics, as is the case for adakites of the present study. Thus, amphiboles allow for estimates of the geochemical features of parental melts in adakitic rocks and, in postcollisional settings, may provide evidence for deep crust. At the same time, amphiboles can also constrain the melt characteristics of these magmas during low-pressure stages, which provide important information constraints on adakite petrogenesis. Although slab or deep crustal melt models for many adakites are rejected in favor of crystal fractionation scenarios [e.g., *Richards and Kerrich*, 2007], our results provide a novel example of the degradation of adakite signatures by crystal fractionation processes.

6. Concluding Remarks

We identify two distinct groups of amphiboles in the Early Permian postcollisional adakitic plutons the Tianshan Orogen, including high- and low-pressure amphiboles. The results show that the melts in equilibrium with the high-pressure amphiboles from the Awulale adakitic rocks already had adakitic characteristics. In contrast, the melts in equilibrium with low-pressure amphiboles do not display adakitic geochemical features. Petrological evidence presented in this study suggests that high-pressure amphibole composition lends new insights to constrain the geochemical characteristics of pristine adakitic magmas. Melting of thickened lower crust can produce pristine adakitic magma, regardless of whether or not the adakitic magmas were produced via crystallization [*Castillo et al*., 1999; *Macpherson et al*., 2006]. Such lower crust-derived adakitic rocks have the potential for tracing the time at which anomalously thick continental crust is developed in settings such as the Tibetan plateau [*Chung et al*., 2003; *Wang et al*., 2005] or the Andes in South America [*Goss and Kay*, 2009].

Acknowledgments
We sincerely thank Editor-in-Chief Michael Walter and Tracy Rushmer and Julia Ribeiro for their constructive and helpful suggestions on the early version of this manuscript. This study was supported by the Strategic Priority Research Program (B) of the Chinese Academy of Sciences (grants XDB03010600 and XDB18020204), the National Natural Science Foundation of China (grants 41202041, 41673033, and 41630208), the Key Program of the Chinese Academy of Sciences (QYZDJ-SSW-DQC026), talent project of Guangdong Province (2014TX01Z079), and GIG-CAS 135 project 135TP201601. This is contribution IS-2361 from GIG-CAS. The data for this paper are available by contacting the corresponding author at tanggj@gig.ac.cn.

References

Adam, J., R. Oberti, F. Cámara, and T. H. Green (2007), An electron microprobe, LAM-ICP-MS and single-crystal X-ray structure refinement study of the effects of pressure, melt-H_2O concentration and fO_2 on experimentally produced basaltic amphiboles, *Eur. J. Mineral.*, *19*(5), 641–655.

Alonso-Perez, R., O. Müntener, and P. Ulmer (2009), Igneous garnet and amphibole fractionation in the roots of island arcs: Experimental constraints on andesitic liquids, *Contrib. Mineral. Petrol.*, *157*(4), 541–558.

Anderson, J. L., and D. R. Smith (1995), The effects of temperature and fO_2 on the Al-in-hornblende barometer, *Am. Mineral.*, *80*(5–6), 549–559.

Anderson, J. L., A. P. Barth, J. L. Wooden, and F. Mazdab (2008), Thermometers and thermobarometers in granitic systems, *Rev. Mineral. Geochem.*, *69*(1), 121–142.

Atherton, M. P., and N. Petford (1993), Generation of sodium-rich magmas from newly underplated basaltic crust, *Nature*, *362*(6416), 144–146.

Bachmann, O., and M. A. Dungan (2002), Temperature-induced Al-zoning in hornblendes of the Fish Canyon magma, Colorado, *Am. Mineral.*, *87*(8–9), 1062–1076.

Bernard, A., D. Demaiffe, N. Mattielli, and R. S. Punongbayan (1991), Anhydrite-bearing pumices from Mount Pinatubo: Further evidence for the existence of sulphur-rich silicic magmas, *Nature*, *354*(6349), 139–140.

Bernard, A., U. Knittel, B. Weber, D. Weis, A. Albrecht, K. H. Hattori, J. Klein, and D. Oles (1996), Petrology and geochemistry of the 1991 eruption products of Mount Pinatubo, in *Fire and Mud: Eruptions and Lahars of Mount Pinatubo, Philippines*, edited by C. G. Newhall and R. S. Punongbayan, pp. 767–797, Univ. of Washington Press, Quezon City: Philippine Institute of Volcanology and Seismology, Seattle, Wash.

Blundy, J. D., and T. J. B. Holland (1990), Calcic amphibole equilibria and a new amphibole-plagioclase geothermometer, *Contrib. Mineral. Petrol.*, *104*(2), 208–224.

Castillo, P. R. (2006), An overview of adakite petrogenesis, *Chin. Sci. Bull.*, *51*(3), 258–268.

Castillo, P. R. (2012), Adakite petrogenesis, *Lithos*, *134–135*, 304–316.

Castillo, P. R., P. E. Janney, and R. U. Solidum (1999), Petrology and geochemistry of Camiguin Island, southern Philippines: Insights to the source of adakites and other lavas in a complex arc setting, *Contrib. Mineral. Petrol.*, *134*(1), 33–51.

Chambefort, I., J. H. Dilles, and A. A. Longo (2013), Amphibole Geochemistry of the Yanacocha Volcanics, Peru: Evidence for Diverse Sources of Magmatic Volatiles Related to Gold Ores, *J. Petrol.*, *54*(5), 1017–1046.

Chung, S. L., D. Y. Liu, J. Q. Ji, M. F. Chu, H. Y. Lee, D. J. Wen, C. H. Lo, T. Y. Lee, Q. Qian, and Q. Zhang (2003), Adakites from continental collision zones: Melting of thickened lower crust beneath southern Tibet, *Geology*, *31*(11), 1021–1024.

Coldwell, B., J. Adam, T. Rushmer, and C. G. Macpherson (2011), Evolution of the East Philippine Arc: Experimental constraints on magmatic phase relations and adakitic melt formation, *Contrib. Mineral. Petrol.*, *162*(4), 835–848.

Davidson, J., S. Turner, H. Handley, C. Macpherson, and A. Dosseto (2007), Amphibole "sponge" in arc crust?, *Geology*, *35*(9), 787–790.

Defant, M. J., and M. S. Drummond (1990), Derivation of some modern arc magmas by melting of young subducted lithosphere, *Nature*, *347*(6294), 662–665.

Ernst, W. G., and J. Liu (1998), Experimental phase-equilibrium study of Al- and Ti-contents of calcic amphibole in MORB; a semiquantitative thermobarometer, *Am. Mineral.*, *83*(9–10), 952–969.

Foley, F. V., N. J. Pearson, T. Rushmer, S. Turner, and J. Adam (2013), Magmatic Evolution and Magma Mixing of Quaternary Adakites at Solander and Little Solander Islands, New Zealand, *J. Petrol.*, *54*(4), 703–744.

Foley, S., M. Tiepolo, and R. Vannucci (2002), Growth of early continental crust controlled by melting of amphibolite in subduction zones, *Nature*, *417*(6891), 837–840.

Foley, S. F., M. G. Barth, and G. A. Jenner (2000), Rutile/melt partition coefficients for trace elements and an assessment of the influence of rutile on the trace element characteristics of subduction zone magmas, *Geochim. Cosmochim. Acta*, *64*(5), 933–938.

Gao, J., R. Klemd, Q. Qian, X. Zhang, J. Li, T. Jiang, and Y. Yang (2011), The collision between the Yili and Tarim blocks of the Southwestern Altaids: Geochemical and age constraints of a leucogranite dike crosscutting the HP–LT metamorphic belt in the Chinese Tianshan Orogen, *Tectonophysics*, *499*(1–4), 118–131.

Goss, A. R., and S. M. Kay (2009), Extreme high field strength element (HFSE) depletion and near-chondritic Nb/Ta ratios in Central Andean adakite-like lavas (~28°S, ~ 68°W), *Earth Planet. Sci. Lett.*, *279*(1–2), 97–109.

Green, T. H. (1982), Anatexis of mafic crust and high pressure crystallization of andesite, in *Andesites: Orogenic Andesites and Related Rocks*, edited by R. S. Thorpe, pp. 465–487, John Wiley, New York.

Hammarstrom, J. M., and E.-a. Zen (1986), Aluminum in hornblende: An empirical igneous geobarometer, *Am. Mineral.*, *71*(11–12), 1297–1313.

Han, B. F., Z. J. Guo, Z. C. Zhang, L. Zheng, J. F. Chen, and B. Song (2010), Age, geochemistry, and tectonic implications of a late Paleozoic stitching pluton in the North Tian Shan suture zone, western China, *Geol. Soc. Am. Bull.*, *122*(3–4), 627–640.

Han, B.-F., G.-Q. He, X.-C. Wang, and Z.-J. Guo (2011), Late Carboniferous collision between the Tarim and Kazakhstan–Yili terranes in the western segment of the South Tian Shan Orogen, Central Asia, and implications for the Northern Xinjiang, western China, *Earth Sci. Rev.*, *109*(3–4), 74–93.

Hidalgo, S., M. Monzier, H. Martin, G. Chazot, J.-P. Eissen, and J. Cotten (2007), Adakitic magmas in the Ecuadorian Volcanic Front: Petrogenesis of the Iliniza Volcanic Complex (Ecuador), *J. Volcanol. Geotherm. Res.*, *159*(4), 366–392.

Hoernle, K., et al. (2008), Arc-parallel flow in the mantle wedge beneath Costa Rica and Nicaragua, *Nature*, *451*(7182), 1094–1097.

Holland, T., and J. Blundy (1994), Non-ideal interactions in calcic amphiboles and their bearing on amphibole-plagioclase thermometry, *Contrib. Mineral. Petrol.*, *116*(4), 433–447.

Irvine, T. N., and W. R. A. Baragar (1971), A guide to the chemical classification of the common volcanic rocks, *Can. J. Earth Sci.*, *8*(5), 523–548.

Jahn, B. M., F. Y. Wu, and B. Chen (2000), Massive granitoid generation in Central Asia: Ndisotope evidence and implication for continental growth in the Phanerozoic, *Episodes*, *23*(2), 82–92.

Johnson, M. C., and M. J. Rutherford (1989), Experimental calibration of the aluminum-in-hornblende geobarometer with application to Long Valley caldera (California) volcanic rocks, *Geology*, *17*(9), 837–841.

Kay, R. W. (1978), Aleutian magnesian andesites: Melts from subducted Pacific ocean crust, *J. Volcanol. Geotherm. Res.*, *4*(1–2), 117–132.

Kay, S. M., E. Godoy, and A. Kurtz (2005), Episodic arc migration, crustal thickening, subduction erosion, and magmatism in the south-central Andes, *Geol. Soc. Am. Bull.*, *117*(1–2), 67–88.

Kiss, B., S. Harangi, T. Ntaflos, P. R. D. Mason, and E. Pál-Molnár (2014), Amphibole perspective to unravel pre-eruptive processes and conditions in volcanic plumbing systems beneath intermediate arc volcanoes: A case study from Ciomadul volcano (SE Carpathians), *Contrib. Mineral. Petrol.*, *167*(3), 986.

Klemme, S., S. Prowatke, K. Hametner, and D. Gunther (2005), Partitioning of trace elements between rutile and silicate melts: Implications for subduction zones, *Geochim. Cosmochim. Acta*, *69*(9), 2361–2371.
Le Maitre, R. W. (2002), *Igneous Rocks: A Classification and Glossary of Terms*, 236 pp., Cambridge Univ. Press, Cambridge, U. K., and New York.
Leake, B. E., et al. (1997), Nomenclature of amphiboles: Report of the Subcommittee on Amphiboles of the International Mineralogical Association, Commission on New Minerals and Mineral Names, *Am. Mineral.*, *82*(9–10), 1019–1037.
Lee, C., and C. Lim (2014), Short-term and localized plume-slab interaction explains the genesis of Abukuma adakite in Northeastern Japan, *Earth Planet. Sci. Lett.*, *396*, 116–124.
Liu, Y. S., Z. C. Hu, S. Gao, D. Günther, J. Xu, C. G. Gao, and H. H. Chen (2008), In situ analysis of major and trace elements of anhydrous minerals by LA-ICP-MS without applying an internal standard, *Chem. Geol.*, *257*(1–2), 34–43.
Macpherson, C. G., S. T. Dreher, and M. F. Thirlwall (2006), Adakites without slab melting: High pressure differentiation of island arc magma, Mindanao, the Philippines, *Earth Planet. Sci. Lett.*, *243*(3–4), 581–593.
Martin, H., R. H. Smithies, R. Rapp, J. F. Moyen, and D. Champion (2005), An overview of adakite, tonalite-trondhjemite-granodiorite (TTG), and sanukitoid: Relationships and some implications for crustal evolution, *Lithos*, *79*(1–2), 1–24.
Peacock, S. M., T. Rushmer, and A. B. Thompson (1994), Partial melting of subducting oceanic-crust, *Earth Planet. Sci. Lett.*, *121*(1–2), 227–244.
Peccerillo, A., and S. R. Taylor (1976), Geochemistry of Eocene calc-alkaline volcanic rocks from the Kastamonu area, Northern Turkey, *Contrib. Mineral. Petrol.*, *58*(1), 63–81.
Prouteau, G., and B. Scaillet (2003), Experimental Constraints on the Origin of the 1991 Pinatubo Dacite, *J. Petrol.*, *44*(12), 2203–2241.
Putirka, K. (2016), Amphibole thermometers and barometers for igneous systems and some implications for eruption mechanisms of felsic magmas at arc volcanoes, *Am. Mineral.*, *101*(4), 841–858.
Qian, Q., and J. Hermann (2013), Partial melting of lower crust at 10–15 kbar: Constraints on adakite and TTG formation, *Contrib. Mineral. Petrol.*, *165*, 1195–1224.
Rapp, R. P., N. Shimizu, and M. D. Norman (2003), Growth of early continental crust by partial melting of eclogite, *Nature*, *425*(6958), 605–609.
Ribeiro, J. M., R. C. Maury, and M. Grégoire (2016), Are adakites slab melts or high-pressure fractionated mantle melts?, *J. Petrol.*, *57*(5), 839–862.
Richards, J. P., and R. Kerrich (2007), Special paper: Adakite-like rocks: Their diverse origins and questionable role in metallogenesis, *Econ. Geol.*, *102*(4), 537–576.
Ridolfi, F., A. Renzulli, and M. Puerini (2010), Stability and chemical equilibrium of amphibole in calc-alkaline magmas: An overview, new thermobarometric formulations and application to subduction-related volcanoes, *Contrib. Mineral. Petrol.*, *160*(1), 45–66.
Rudnick, R. L., and S. Gao (2003), The composition of the continental crust, in *The Crust*, edited by R. L. Rudnick, pp. 1–64, Elsevier–Pergamon, Oxford.
Samaniego, P., C. Robin, G. Chazot, E. Bourdon, and J. Cotten (2010), Evolving metasomatic agent in the Northern Andean subduction zone, deduced from magma composition of the long-lived Pichincha volcanic complex (Ecuador), *Contrib. Mineral. Petrol.*, *160*(2), 239–260.
Scaillet, B., and B. W. Evans (1999), The 15 June 1991 Eruption of Mount Pinatubo. I. Phase Equilibria and Pre-eruption P–T–fO2–fH2O Conditions of the Dacite Magma, *J. Petrol.*, *40*(3), 381–411.
Schmidt, M. W. (1992), Amphibole composition in tonalite as a function of pressure: An experimental calibration of the Al-in-hornblende barometer, *Contrib. Mineral. Petrol.*, *110*(2), 304–310.
Sisson, T. W. (1994), Trace-element partitioning with application to magmatic processes hornblende-melt trace-element partitioning measured by ion microprobe, *Chem. Geol.*, *117*(1), 331–344.
Sun, S. S., and W. F. McDonough (1989), Chemical and isotopic systematics of oceanic basalts: Implications for mantle composition and processes, in *Magmatism in the Ocean Basins*, *Geol. Soc. Spec. Publ.*, vol. 42, edited by A. D. Saunders and M. J. Norry, pp. 313–345.
Sun, W.-D., M.-X. Ling, S.-L. Chung, X. Ding, X.-Y. Yang, H.-Y. Liang, W.-M. Fan, R. Goldfarb, and Q.-Z. Yin (2012), Geochemical constraints on adakites of different origins and copper mineralization, *J. Geol.*, *120*(1), 105–120.
Tang, G. J., Q. Wang, D. A. Wyman, Z. X. Li, Z. H. Zhao, X. H. Jia, and Z. Q. Jiang (2010), Ridge subduction and crustal growth in the Central Asian Orogenic Belt: Evidence from Late Carboniferous adakites and high-Mg diorites in the western Junggar region, northern Xinjiang (west China), *Chem. Geol.*, *227*(3–4), 281–300.
Tiepolo, M., R. Oberti, A. Zanetti, R. Vannucci, and S. F. Foley (2007), Trace-element partitioning between amphibole and silicate melt, *Rev. Mineral. Geochem.*, *67*(1), 417–452.
Tu, X. L., H. Zhang, W. F. Deng, M. X. Ling, H. Liang, Y. Liu, and W. D. Sun (2011), Application of RESOlution in-situ laser ablation ICP-MS in trace element analyses, *Geochimica*, *40*(1), 83–98.
Wang, Q., F. McDermott, J. F. Xu, H. Bellon, and Y. T. Zhu (2005), Cenozoic K-rich adakitic volcanic rocks in the Hohxil area, northern Tibet: Lower-crustal melting in an intracontinental setting, *Geology*, *33*(6), 465–468.
Xiong, X. L., J. Adam, and T. H. Green (2005), Rutile stability and rutile/melt HFSE partitioning during partial melting of hydrous basalt: Implications for TTG genesis, *Chem. Geol.*, *218*(3–4), 339–359.
Xiong, X. L., X. C. Liu, Z. M. Zhu, Y. Li, W. S. Xiao, M. S. Song, S. Zhang, and J. H. Wu (2011), Adakitic rocks and destruction of the North China Craton: Evidence from experimental petrology and geochemistry, *Sci. China Earth Sci.*, *54*(6), 858–870.
Zhao, Z. H., X. L. Xiong, Q. Wang, D. A. Wyman, Z. W. Bao, Z. H. Bai, and Y. L. Qiao (2008), Underplating-related adakites in Xinjiang Tianshan, China, *Lithos*, *102*(1–2), 374–391.